British Journal of Pharmacology (2005) 145, 313–322
www.nature.com/bjp

Antagonism of ATP responses at P2X receptor subtypes by the pH indicator dye, Phenol red

*,[1]Brian F. King, [2,6]Min Liu, [3]Andrea Townsend-Nicholson, [4]Jürg Pfister, [4]Fernando Padilla, [4]Anthony P. Ford, [4]Joel R. Gever, [4]Ian B. Oglesby, [5]Stephanie Schorge & [2]Geoffrey Burnstock

[1]University College London, Department of Physiology, Royal Free Campus, Rowland Hill Street, Hampstead, London NW3 2PF; [2]University College London, Department of Anatomy and Developmental Biology, Autonomic Neurosciences Institute, Rowland Hill Street, Hampstead, London NW2 3PF; [3]University College London, Department of Biochemistry and Molecular Biology, Gower Street, London WC1E 6BT; [4]Roche Palo Alto LLC, 3431 Hillview Avenue, Palo Alto, CA 94304, U.S.A. and [5]University College London, Institute of Neurology, Queen's Square, London WC1N 4BG

1 Many types of culture media contain a pH-sensitive dye. One commonly occurring dye, Phenol red sodium (Na^+) salt, was tested for blocking activity at rat $P2X_{1-4}$ receptors ($P2X_{1-4}Rs$) expressed in *Xenopus* oocytes.

2 Phenol red Na^+-salt antagonised adenosine 5′-triphosphate (ATP) responses at $P2X_1R$ (IC_{50}, 3 μM) and, at higher concentrations, also blocked $P2X_2R$ and $P2X_3R$. Phenol red Na^+-salt, purified of lipophilic contaminants, blocked $P2X_1R$ and $P2X_3R$ by acting as an insurmountable antagonist.

3 Two lipophilic extracts of Phenol red antagonised ATP responses at P2XRs. Extract A was a potent antagonist at $P2X_1R$ (IC_{50}, 1.4 μM), whereas extract B was a potent antagonist at $P2X_3R$ (IC_{50}, 4.1 μM). A bisphenolic compound (RS151030) found in these extracts was a potent antagonist at $P2X_1R$ (IC_{50}, 0.3 μM) and at $P2X_3R$ (IC_{50}, 2.4 μM).

4 Phenolphthalein base was a potent irreversible antagonist at $P2X_1R$ (IC_{50}, 1 μM), whereas Phenolphthalein K^+-salt was 25-fold less potent here.

5 Phenolphthalein base was a reversible antagonist of ATP responses at rat $P2X_4R$ (IC_{50}, 26 μM), whereas Phenolphthalein K^+-salt was inactive.

6 Dimethyl sulphoxide (DMSO), used to dissolve lipophilic extracts, showed pharmacological activity by itself at rat $P2X_1R$ and $P2X_4R$.

7 Thus, Phenol red and related compounds are antagonists at rat $P2X_1R$, but are also active at other rat P2XRs. Phenolphthalein base is a newly identified, low potency antagonist of ATP responses at $P2X_4R$. Culture media containing these red dyes should be used cautiously in future pharmacological studies of P2XRs. Also, wherever possible, the solvent DMSO should be used with caution.
British Journal of Pharmacology (2005) **145,** 313–322. doi:10.1038/sj.bjp.0706187
Published online 21 March 2005

Keywords: Purinoceptor; P2X receptor; ion-channel; ATP; Phenol red; Phenolphthalein; antagonism

Abbreviations: 1321-N1 cells, human astrocytoma cell line; α,βmeATP, alpha,beta-methyleneATP; ATP, adenosine 5′-triphosphate; CHO-K1, Chinese hamster ovary, K1 cell line; DMEM, Dulbecco's modified Eagle medium; DMSO, dimethyl sulphoxide; DRG cells, dorsal root ganglion cells; FLIPR, fluorimetric imaging plate reader; HEK 293, human embryonic kidney 293 cells; J774 cells, mouse macrophage cell line; LGIC, ligand-gated ion-channel; MDCK cells, Madin–Darby canine kidney cells; nAChR, nicotinic acetylcholine receptor; n_H, Hill coefficient; PR, Phenol red (phenolsulphonephthalein sodium (Na^+) salt); P2XR, P2X receptor; V_h, holding potential

Introduction

P2X receptors (P2XRs) are ligand-gated ion-channels (LGICs) that are widely distributed among various tissue types, including neurons, retinal cells, glia, cardiac and smooth muscles, secretory epithelia, haemopoietic cells and blood platelets (Khakh *et al*., 2001; North, 2002). P2XRs are activated by extracellular adenosine 5′-triphosphate (ATP) and, when activated, affect their host cell in three well-defined ways: (i) influx of extracellular sodium ions to cause depolarisation; (ii) influx of extracellular calcium ions to activate intracellular mechanisms; (iii) for the $P2X_7R$ subtype in particular, channel-to-pore conversion with the loss of size- and charge-selectivity for channel permeants (Khakh *et al*., 2001; North, 2002).

Seven subunits are involved in the construction of mammalian P2XRs – the $P2X_1$ to $P2X_7$ proteins. Each subunit is capable of forming functional homomeric assemblies, which comprise three identical externally glycosylated proteins (Nicke *et al*., 1998; Rettinger *et al*., 2000; Khakh *et al*., 2001; North, 2002; Jiang *et al*., 2003; Aschrafi *et al*., 2004). The number of functional homomeric P2XRs in a cell appears to depend on the trafficking efficiency of P2X subunits from the

*Author for correspondence; E-mail: b.king@rfc.ucl.ac.uk
[6]Current address: Department of Pharmacology and Clinical Pharmacology, St George's Hospital Medical School, Cranmer Terrace, London SW17 0RE, U.K.
Published online 21 March 2005

endoplasmic reticulum to the membrane (Collo *et al*., 1996; North, 2002; Aschrafi *et al*., 2004) although, for $P2X_6R$, it also depends on the efficiency of subunit glycosylation (Jones *et al*., 2004). Thus, studies of homomeric $P2X_{1-4}R$ subtypes are relatively straightforward because these four subtypes are expressed well in all heterologous systems (Khakh *et al*., 2001; North, 2002). On the other hand, homomeric $P2X_5R$ and $P2X_6R$ subtypes are difficult to study because the number of functional receptors on the cell surface is exceedingly low in all expression systems tested (Collo *et al*., 1996; King *et al*., 2000; North, 2002; Wildman *et al*., 2002; Aschrafi *et al*., 2004; Jones *et al*., 2004). The $P2X_7R$ subtype is expressed well in the oocyte expression system, but this receptor is difficult to control pharmacologically once the channel-to-pore transition has been initiated (Nuttle & Dubyak, 1994).

It is now a feature of modern pharmacological investigations to study P2XRs either in primary cultures of acutely dissociated cells (e.g. DRG, neuronal, platelet, retinal and smooth muscle cells), or in secondary cultures of immortalised cells (e.g. MDCK and J774 cells), or as recombinant protein assemblies expressed in mammalian cell types (e.g. CHO-K1, HEK 293 and 1321-N1 astrocytoma cells)). In many cases, cells are bathed in culture media containing the pH indicator dye, Phenol red sodium (Na^+) salt. The concentration of this agent varies from 3 to 50 μM in culture media (based on the dye content of commercially available media), such as Ham (F10 or F12) solution (3 μM); Roswell Park Memorial Institute (RPMI) medium (12 μM); basal medium Eagle (BME, 25 μM); minimum essential medium (MEM; 25 μM); Hank's balanced salt solution (30 μM); Dulbecco's modified Eagle medium (DMEM, 35 μM) and medium 199 (50 μM); Connaught Medical Research Lab (CMRL) medium (50 μM).

The notion that Phenol red Na^+-salt might exert pharmacological actions at ligand-gated membrane receptors such as the P2XR family has not been explored until now, although this pH indicator dye does not noticeably affect voltage-gated Na^+-, K^+- and Ca^{2+}-selective ion-channels in squid axon (Mullins *et al*., 1983). However, lipophilic impurities of Phenol red are known to affect cation transporters in some cell types (Hopp & Bunker, 1993; Kym *et al*., 1996) and to antagonise thromboxane-A_2 receptors in human platelets and canine arteries (Greenberg *et al*., 1994). Additionally, lipophilic impurities in Phenol red have either cytotoxic or oestrogenic/proliferative actions at a number of primary and secondary cell cultures (Berthois *et al*., 1986; Bindal *et al*., 1988; Ernst *et al*., 1989; Grady *et al*., 1991; Raam, 1992). Here, we report the blocking actions of commercially available Phenol red Na^+-salt – and several related compounds – on recombinant isoforms of rat $P2X_{1-4}R$ subtypes at drug concentrations relevant to cell culture conditions. Part of this study has appeared in Abstract form (King *et al*., 2003).

Methods

Oocyte preparation

Xenopus laevis frogs were anaesthetised in Tricaine (0.4% $w\,v^{-1}$), killed by decapitation and the ovarian lobes removed surgically. Isolated oocytes (stages V and VI) were treated with collagenase (Type IA, 2 mg ml^{-1} in a Ca^{2+}-free Ringer's solution, for 2 h) to break down the follicle cell layer that envelops each oocyte. Thereafter, oocytes were shrunk using a double-strength, hyperosmotic Ca^{2+}-free Ringer's solution and the loosely adherent follicle cell layer was removed using fine forceps. Freshly prepared defolliculated oocytes were stored in Barth's solution (pH 7.50) containing NaCl, 110 mM; KCl, 1 mM; Tris-HCl, 7.5 mM; $Ca(NO_3)_2$, 0.33 mM; $CaCl_2$, 0.41 mM; $MgSO_4$, 0.82 mM; $NaHCO_3$, 2.4 mM; gentamycin sulphate, 50 $\mu g\,l^{-1}$. Defolliculated oocytes do not possess functional adenosine and ATP receptors (King *et al*., 1996a, b). Also, these large single cells are deficient in cell-surface ATPases (Ziganshin *et al*., 1995) that are often inhibited by P2 receptor antagonists (Ziganshin *et al*., 1996).

Electrophysiological recordings

cRNA (40 nl, 1 $\mu g\,\mu l^{-1}$) for either rat $P2X_1R$, $P2X_2R$, $P2X_3R$ or $P2X_4R$ was injected into the cytosol of defolliculated oocytes. Injected oocytes were left for 48 h at 18°C in Barth's solution and, thereafter, kept for up to 7 days at 4°C in Barth's solution until used in electrophysiological experiments. ATP-activated membrane currents (I_{ATP}) were recorded from cRNA-injected oocytes using twin microelectrode, voltage-clamp techniques (Axoclamp 2A & 2B amplifiers; Axon Instruments, Union City, CA, U.S.A.). The voltage- and current-recording microelectrodes (0.5–2.0 MΩ) were filled with a filtered 3 M KCl solution. Oocytes were placed in a recording chamber (0.5 ml capacity) and superfused (5 ml min^{-1}) with a Ringer's solution (18°C; adjusted to pH 7.50 with either NaOH or HCl) containing NaCl, 110 mM; KCl, 2.5 mM; HEPES, 5 mM and $BaCl_2$, 1.8 mM. Recordings were stored on magnetic tapes using a DAT recorder (Sony 1000ES) and displayed on a *WindoGraf 900* thermal array recorder (Gould Nicolet Technologies, Ilford, Essex, U.K.).

Drug actions

In oocyte experiments, recombinant P2XRs were activated by extracellular ATP, which was applied for 60 s or until evoked currents reached their peak amplitude. ATP was reapplied after a period of 20 min washout, an interapplication interval that provided agonist responses of identical amplitude (Wildman *et al*., 1999) and twice as long as the time needed for internalised P2X subunit proteins to return to the cell surface (Ennion & Evans, 2001). Agonist concentration/response curves were constructed by using increasing concentrations of ATP and normalising evoked responses to the maximum current elicited by ATP. EC_{50} values for ATP were determined from Hill plots of the transform ($I/I_{max}-I$), where I is the peak current evoked by each ATP concentration. Values of the Hill coefficient (n_H) were also taken from these transforms. Graphs were drawn using *Prism* v2.0 (GraphPad Software, San Diego, CA, U.S.A.), and significant statistical differences between data points were determined by Student's *t*-test (using *Instat* v2.05A, GraphPad).

Antagonists were applied for 20 min prior to, and during, the application of the agonist ATP. Here, ATP was used at the approximate EC_{75} concentration: $P2X_1R$, 3 μM; $P2X_2R$, 30 μM; $P2X_3R$, 3 μM; $P2X_4R$, 10 μM. Increasing concentrations of antagonists were applied and the degree of inhibition of ATP responses determined by normalising data to the mean current of three control applications of ATP (at the EC_{75} concentration) in the absence of the antagonist. Inhibition curves were

drawn using *Prism* v2.0 (GraphPad). Data are presented as the mean ± s.e.m. of four sets of results from different batches of defolliculated oocytes.

Fluorimetric Ca^{2+}-imaging analysis

CHO-K1 cells stably expressing either human $P2X_1R$ or rat $P2X_3R$ subunits, or 1321N1 human astrocytoma cells stably expressing human $P2X_3R$ subunits, were used in fluorimetric Ca^{2+}-imaging experiments. At 18–24 h prior to use, cells were seeded into black-walled 96-well plates at a density of 50,000 cells well^{-1} and incubated overnight (5% CO_2, 95% relative humidity, at 37°C) in a Phenol red-free nutrient medium (Ham F-12; Invitrogen, Carlsbad CA, U.S.A.). Prior to use, cells were washed in a buffer (FLIPR buffer (FB): magnesium-free Hank's balanced salt solution, supplemented with HEPES, 10 mM; $CaCl_2$, 2 mM; probenecid, 2.5 mM), and then loaded with a Ca^{2+}-sensitive fluorescent dye (Fluo-3 AM, 2 μM final concentration; at 37°C). After 1 h incubation, cells were washed four times with FB, and a final volume of 75 μl well^{-1} left in each well. Antagonists, or vehicle, were added to each well (25 μl of a 4 × solution) and allowed to equilibrate for 60 min at room temperature. Plates were placed in a FLIPR (*Fluorimetric Imaging Plate Reader*; Molecular Devices, Sunnyvale CA, U.S.A.), and baseline fluorescence was measured (excitation, 488 nm; emission, 510–570 nm) for 10 s before the addition of the agonist α,βmeATP ($P2X_1R$, 0.1 μM; $P2X_3R$, 1 μM; 100 μl well^{-1}). Fluorescence was measured every 1 s for 120 s after agonist addition. Peak fluorescence in response to the addition of α,βmeATP was measured in both the absence and presence of antagonists.

Whole-cell recordings from CHO-r$P2X_3$ cells

Whole-cell recordings were made under voltage-clamp conditions from CHO-K1 cells stably expressing rat $P2X_3$ subunits. Cells were plated onto poly-D-Lysine coated coverslips and incubated in a growth medium (L-15) for 1–4 days at 37°C. Recordings were made using an Axopatch-IC amplifier (Axon Instruments, Foster City CA, U.S.A.), with cells held at −60 mV. Recording electrodes (resistance 1–4 MΩ) were filled with an intracellular solution containing KCl, 120 mM; HEPES, 10 mM; potassium citrate, 10 mM; pH 7.2. CHO-r$P2X_3$ cells were superfused with Dulbecco's phosphate-buffered saline (supplemented with $CaCl_2$, 1 mM; $MgCl_2$, 0.5 mM). Data were acquired using pCLAMP 9 software (Axon Instruments) and signals were filtered at 2 kHz (−3 dB frequency, Bessel filter, 80 dB decade^{-1}). Drugs (5 mM stock solution diluted in extracellular buffer) were delivered by gravity flow and regulated by a *Valvebank II* system (Automate Scientific, San Francisco CA, U.S.A.). CHO-r$P2X_3R$ cells were activated with $\alpha\beta$meATP (10 μM, 3 s every 4 min) until reproducible inward currents were obtained. Thereafter, CHO-r$P2X_3$ cells were superfused with Phenol red Na^+-salt (in extracellular buffer) for 4 min followed by $\alpha\beta$meATP (10 μM, 3 s). After washout (4 min), cells were challenged again with $\alpha\beta$meATP (10 μM, 3 s).

Whole-cell recordings from HEK 293 cells

HEK 293 cells were maintained in Phenol red-free DMEM (Sigma-Aldrich Chemical Co., Poole, Dorset, U.K.) and transiently transfected, as described in Schorge & Colquhoun (2003), with the rat $P2X_1$ receptor cDNA. A reporter gene, green fluorescent protein (GFP), was also included in transfections to identify cells for whole-cell voltage-clamp experiments. At 3 days post-transfection, $\alpha\beta$meATP (1 μM) evoked inward currents were recorded from HEK 293 cells using the whole-cell recording conditions described in Valera *et al.* (1994). The agonist was applied *via* a Y-tube positioned close to GFP-labelled cells (< 100 μm). When used, Phenol red Na^+-salt was applied for at least 30 min prior to recording at a concentration of 100 μM.

Drug purification and solutions

Phenol red (phenolsulphonephthalein sodium (Na^+) salt), Phenolphthalein base (3,3-*bis*[4-hydroxyphenol]-1(*3H*)-isobenzofuranone) and Phenolphthalein disulphate potassium salt (Figure 1) were obtained from Sigma-Aldrich Chemical Co. (Poole, Dorset U.K.). Phenol Red (listed as 90% pure) was cleared of lipophilic impurities by an earlier, established method (Bindal *et al.*, 1988; Grady *et al.*, 1991). Briefly, commercially available Phenol red was partitioned between water and diethyl-ether and the two phases separated. Excess ether was removed from the aqueous phase under vacuum. The nonaqueous phase was concentrated, dried and the residue redissolved in ethanol. Separation by reverse-phase HPLC yielded two major lipophilic extracts (A and B) (Grady *et al.*, 1991; Kym *et al.*, 1996). One compound known to be present

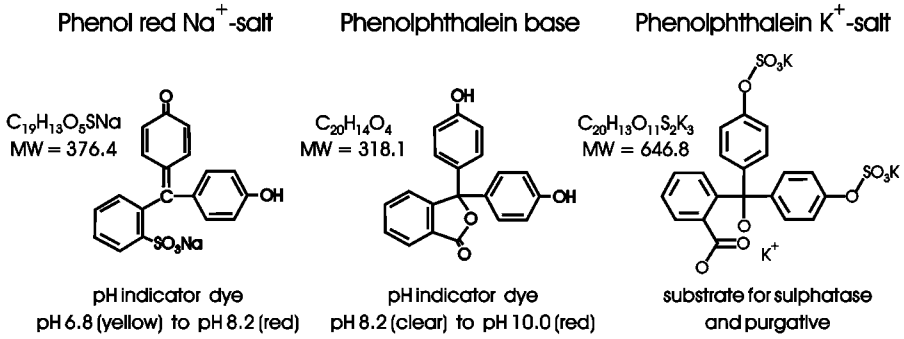

Figure 1 Chemical formula, molecular weight and structure of the pH-sensitive dyes, *Phenol red* sodium salt, *Phenolphthalein* base and *Phenolphthalein disulphate* potassium salt.

in these lipophilic extracts – *Compound 5* (9,9-*bis*[4-hydroxyphenol]-3-hydroxyfluorene) and, here, renamed RS151030 – was synthesised *de novo* according to an earlier specified protocol (Kym *et al*., 1996).

ATP (adenosine 5′-triphosphate disodium salt) was obtained from Sigma-Aldrich Chemical Co. (Poole, Dorset). Other chemicals were Analar grade from Sigma-Aldrich. ATP and Phenol red sodium salt were dissolved in a Ca^{2+}-free Ringer's solution (pH 7.50). Phenolphthalein base and lipophilic extracts of Phenol red were dissolved in dimethyl sulphoxide (DMSO) to give stock solutions of 10 mM and, thereafter, diluted with Ringer's solution to give a range of drug concentrations (0.1–100 μM), which also contained a small – yet pharmacologically active – amount of DMSO (0.001–1% v v^{-1}) (see below).

Results

Blockade by phenol red

Unless stated otherwise, ATP was used in all experiments at the approximate EC_{75} concentration: $P2X_1R$, 3 μM; $P2X_2R$, 30 μM; $P2X_3R$, 3 μM; $P2X_4R$, 10 μM. Commercially available Phenol red Na^+-salt (100 μM) blocked ATP responses at the rat isoform of homomeric $P2X_1R$, $P2X_2R$ and $P2X_3R$, but was not active at $P2X_4R$ (Figure 2a). Phenol red antagonism at these three P2XR subtypes was concentration-dependent (Figure 2b). At $P2X_1R$, the threshold concentration for receptor blockade by Phenol red was 0.3 μM, with full blockade at 100 μM. At $P2X_3R$, the antagonist was approximately 10-fold less potent; the threshold concentration for blockade was 3 μM and full blockade occurred at 1 mM. At $P2X_2R$, the inhibition curve was steep with the threshold concentration for blockade at 30 μM and full blockade at 300 μM. The IC_{50} values (mean $\pm$ s.e.m., $n=4$), and n_H values, for inhibition curves were: $P2X_1R$, 3.0 ± 0.6 μM ($n_H=-1.0\pm0.2$); $P2X_2R$, 51.9 ± 7.8 μM ($n_H=-1.6\pm0.2$); $P2X_3R$, 24.3 ± 4.4 μM ($n_H=-0.9\pm0.2$). At $P2X_4R$, Phenol red was inactive at concentrations up to 100 μM. Phenol red was not tested at $P2X_5$, $P2X_6$ or $P2X_7$ receptors.

After removing lipophilic constituents with diethyl-ether, purified Phenol red Na^+-salt still blocked ATP responses at $P2X_1$ and $P2X_3$ receptors (Figure 3a, b). There was no significant difference between the blocking activities of either purified or commercial Phenol red. IC_{50} (and n_H) values for the purified salt were $P2X_1R$, 2.9 ± 0.5 μM ($n_H=-1.0\pm0.2$); $P2X_3R$, 27.6 ± 6.8 μM ($n_H=-0.8\pm0.2$). The purified salt was also tested against the ATP concentration–response relationship for $P2X_1$ and $P2X_3$ receptors to determine the nature of receptor blockade (Figure 3c, d). At $P2X_1R$, Phenol red (PR: 0, 1, 3 and 10 μM) suppressed the maximum ATP activity without significantly altering the EC_{50} value for ATP (mean $\pm$ s.e.m., $n=4$): control, 1.0 ± 0.1 μM; PR 1 μM, 0.7 ± 0.1 μM; PR 3 μM, 0.4 ± 0.1 μM; PR 10 μM, 0.4 ± 0.1 μM. At $P2X_3R$, Phenol red (PR: 0, 10, 30 and 100 μM) suppressed the maximum ATP activity without significantly altering ATP potency (mean $\pm$ s.e.m., $n=4$): control, 0.8 ± 0.2 μM; PR 10 μM, 1.1 ± 0.4 μM; PR 30 μM, 0.4 ± 0.1 μM; PR 100 μM, 0.5 ± 0.1 μM. Thus, Phenol red acted as a noncompetitive antagonist at these two P2XR subtypes.

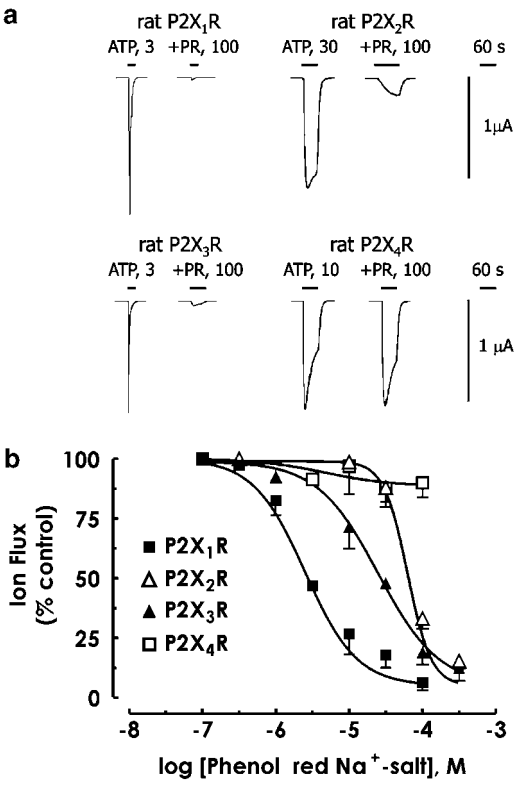

Figure 2 Whole-cell inward currents (in a) evoked by ATP (given at the EC_{75}, in μM) at rat isoforms of P2XR subtypes were antagonised by Phenol red Na^+-salt (PR, 100 μM) at $P2X_1R$, $P2X_2R$ and $P2X_3R$ but not $P2X_4R$. P2XRs were expressed in *Xenopus* oocytes, which were held under voltage-clamp conditions ($V_h=-60$ mV; each pair of records from the same cell). Inhibition curves (in b) for Phenol red Na^+-salt antagonism of ATP responses at four P2XRs, with ATP used at the EC_{75} concentration ($P2X_1R$, 3; $P2X_2R$, 30; $P2X_3R$, 3; $P2X_4R$, 10 μM). Data points are given as mean $\pm$ s.e.m. ($n=4$).

$P2X_1$ and $P2X_3$ receptors were in contact with purified Phenol red Na^+-salt for several hours while constructing concentration–response curves for ATP. Thus, antagonist data were analysed further to reassess the degree of blockade of ATP at the EC_{75} value (3 μM) and to see if there was a use-dependency for the antagonist (Figure 3e, f). For these inhibition curves, antagonism maxima and minima were estimated from earlier inhibition curves. The resultant IC_{50} (and n_H) values were (mean $\pm$ s.e.m., $n=4$): $P2X_1R$, 1.0 ± 0.1 μM ($n_H=-0.8\pm0.1$); $P2X_3R$, 17.3 ± 2.2 μM ($n_H=-1.3\pm0.2$). Here, the IC_{50} value for Phenol red at $P2X_1R$ was significantly lower ($P<0.05$), and this increased potency supports the likelihood of use- and time-dependent block with this drug.

Blockade by Phenolphthalein base

Commercially available Phenolphthalein base blocked ATP responses at the rat $P2X_1R$, $P2X_3R$ and $P2X_4R$, but was much less effective at blocking $P2X_2R$ (Figure 4a, c). Antagonism at these P2XR subtypes was concentration-dependent. At $P2X_1R$, the threshold concentration for receptor blockade was 0.1 μM, with full blockade at 100–300 μM. At $P2X_3R$, the antagonist was approximately 10-fold less potent; the

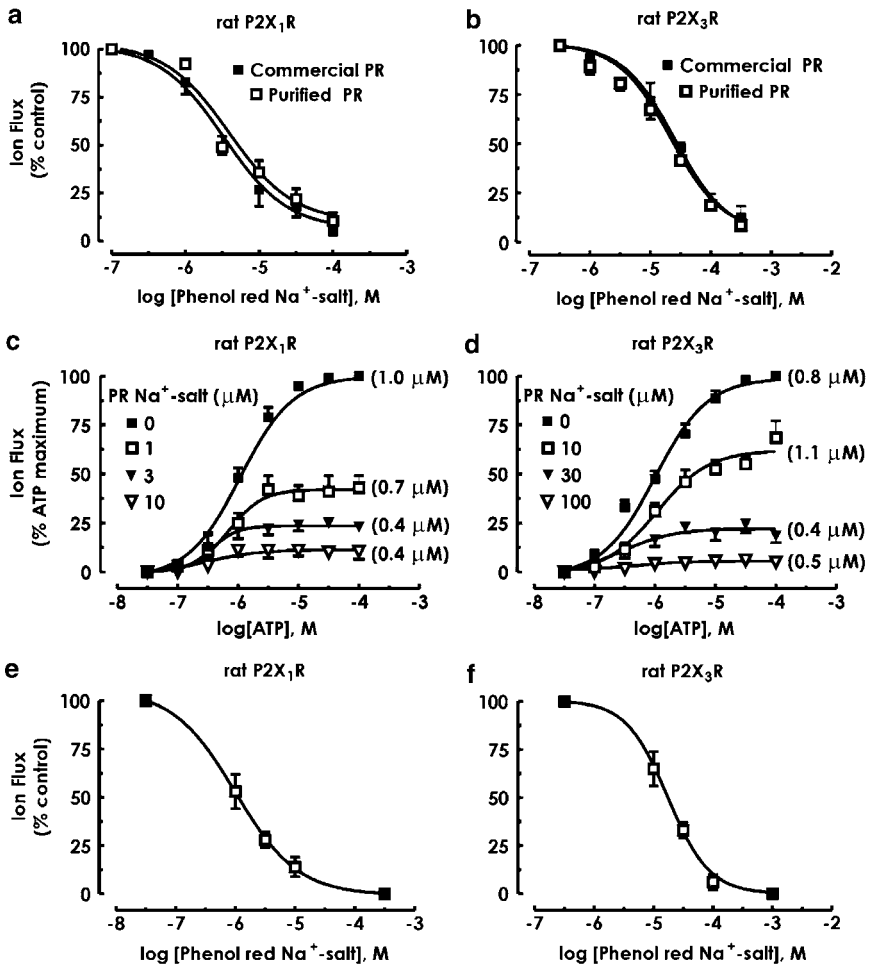

Figure 3 Inhibition curves for commercially available and purified Phenol red Na^+-salt (PR) at the rat isoform of $P2X_1R$ (in a) and $P2X_3R$ (in b). Purified PR was tested for noncompetitive antagonism of responses to extracellular ATP (3 μM, the EC_{75}) at $P2X_1R$ (in c) and $P2X_3R$ (in d). In (c) and (d), data in parentheses give the mean EC_{50} values for ATP with the stated concentrations of purified PR present. Inhibition curves for purified PR at $P2X_1R$ (in e) and $P2X_3R$ (in f) were redrawn from data in (c) and (d) using the data for 3 μM ATP (EC_{75} value). Additionally, maxima and minima (filled symbols) for the inhibition curves in (e) and (f) were taken from earlier data in (a) and (b). All data points are expressed as mean $\pm$ s.e.m. ($n=4$).

threshold concentration for blockade was 1 μM and full blockade occurred at 300 μM. At $P2X_4R$, the inhibition curve was steep – with the threshold concentration for blockade at 2 μM and full blockade at 300 μM. In contrast to Phenol red Na^+-salt experiments, Phenolphthalein base was a very weak antagonist at the $P2X_2$ receptor. The IC_{50} (and n_H) values for inhibition curves were (mean $\pm$ s.e.m., $n=4$): $P2X_1R$, 1.7 ± 0.3 μM ($n_H=-0.7\pm0.2$); $P2X_3R$, 17.9 ± 5.2 μM ($n_H=-0.8\pm0.2$); $P2X_4R$, 25.9 ± 4.7 μM ($n_H=-1.7\pm0.5$). At $P2X_2R$, the IC_{50} value for Phenolphthalein base was estimated as greater than 200 μM.

Phenolphthalein base is water insoluble and, therefore, it was necessary to use the nonaqueous DMSO as a solvent. Control experiments with this vehicle showed that P2XRs were, to varying degrees, sensitive to DMSO (Figure 4b). $P2X_1R$ was most sensitive showing up to 25% reduction of the amplitude of ATP responses with dilutions of 0.01–1.0% ($v\,v^{-1}$) of DMSO in Ringer's solution. $P2X_2R$ and $P2X_3R$ were less sensitive and showed less than 10% reduction of ATP responses over the same range of dilutions. $P2X_4Rs$ showed a modest potentiation of ATP responses – by about 15% – using high dilutions (0.001–0.01%) of DMSO, and this effect declined as lesser dilutions were tested. Since Phenolphthalein base was made up as stock solutions of 10 mM, the subsequent reduction of antagonist stocks to a concentration of 100 μM meant that these solutions contained 1% DMSO, whereas an antagonist concentration of 0.1 μM contained 0.001% DMSO.

The inhibition curves for Phenolphthalein base at $P2X_{1-4}Rs$ were reanalysed and redrawn, using a subtractive process to take into account the effect of DMSO at each dilution factor (Figure 4c). Here, this process involved subtracting the mean amplitude of the potentiating or inhibitory effects of DMSO (as a percentage of control response) from the data for Phenolphthalein base. Under these circumstances, IC_{50} values were (mean $\pm$ s.e.m., $n=4$): $P2X_1R$, 1.0 ± 0.2 μM; $P2X_3R$, 17.9 ± 5.2 μM; $P2X_4R$, 25.8 ± 5.4 μM; $P2X_2R$, >200 μM. None of these IC_{50} values were significantly different from the original determinations.

P2XRs were tested for the recovery of agonist activity from Phenolphthalein base antagonism after a 40-min period of drug washout (Figure 5). For $P2X_1R$, Phenolphthalein (100 μM) blockade was irreversible with only a 5.9 ± 1.1%

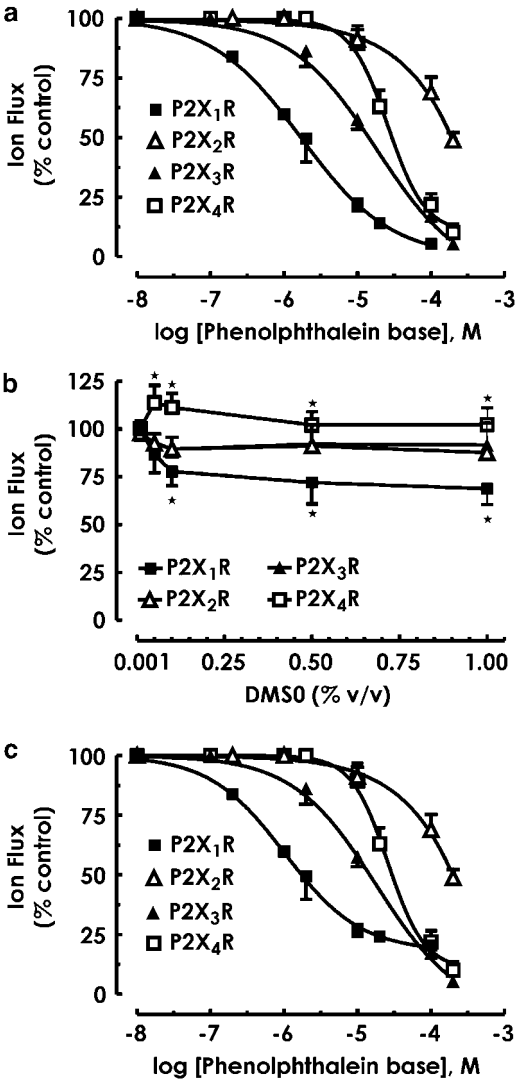

Figure 4 Inhibition curves (in a) for Phenolphthalein base antagonism of ATP responses at rat isoforms of four P2XRs, with ATP used at the EC75 concentration ($P2X_1R$, 3; $P2X_2R$, 30; $P2X_3R$, 3; $P2X_4R$, 10 μM). In (b), the effects of DMSO alone (0.001–1.0% v v^{-1}) on ATP responses at four P2XRs. In (c), inhibition curves for Phenolphthalein base were reanalysed and redrawn using a subtractive process to take into account the effects of DMSO. All data points are expressed as mean $\pm$ s.e.m. ($n=4$); $^*P<0.05$.

($n=4$) recovery of ATP responses. For $P2X_3R$, Phenolphthalein (100 μM) blockade was slowly reversible with $46.2\pm6.0\%$ ($n=4$) recovery of ATP responses (data not shown). For $P2X_4R$, blockade by Phenolphthalein base (200 μM) was reversible with $93.4\pm11.2\%$ ($n=4$) recovery.

Blockade by Phenolphthalein salt

Phenolphthalein disulphate potassium (K^+) salt (Figure 1c) was tested at $P2X_{1-4}$Rs for blocking activity (Figure 6). At the $P2X_1R$, ATP responses were blocked by this compound with an IC_{50} value of 26.1 ± 3.2 μM ($n_H=-0.6\pm0.3$) (mean $\pm$ s.e.m., $n=4$). The IC_{50} values for $P2X_2R$ and $P2X_3R$ were estimated as in excess of 200 μM, whereas the compound was not active at $P2X_4R$.

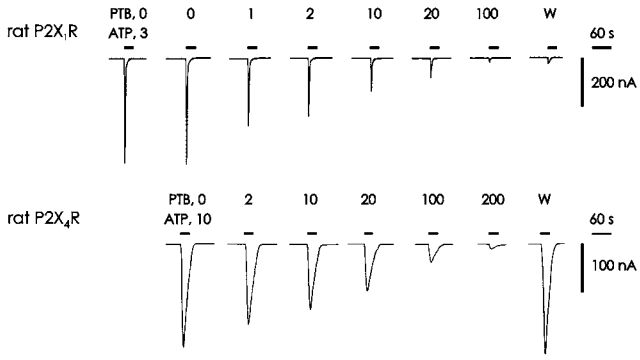

Figure 5 Whole-cell currents inward currents evoked by ATP (given at the EC_{75}, in μM; $P2X_1R$, 3; $P2X_4R$, 10) at the rat isoform of $P2X_1R$ (upper records) and $P2X_4R$ (lower records). At $P2X_1R$, ATP responses were antagonised in an irreversible manner by Phenolphthalein base (PTB, 0–100 μM). At $P2X_4R$, ATP responses were antagonised in a reversible manner by PTB (2–200 μM). Recovery from PTB antagonism was tested after a 40-min period of drug washout (W). Each set of records is from separate cells, held under voltage-clamp ($V_h=-60$ mV).

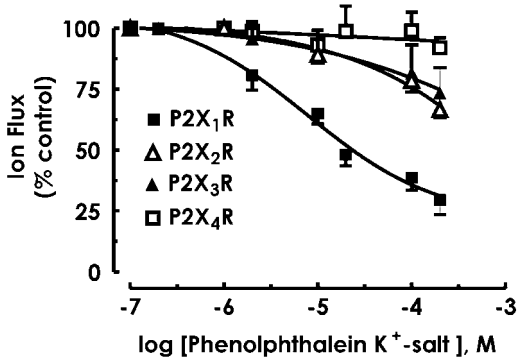

Figure 6 Inhibition curves for Phenolphthalein K^+-salt antagonism of ATP responses at rat isoforms of four P2XRs, with ATP used at the EC_{75} concentration ($P2X_1R$, 3; $P2X_2R$, 30; $P2X_3R$, 3; $P2X_4R$, 10 μM). All data points are expressed as mean $\pm$ s.e.m. ($n=4$).

Blockade by lipophilic extracts of Phenol red

HPLC analysis of lipophilic extracts of Phenol red has revealed two major peaks (Grady *et al*., 1991; Kym *et al*., 1996) and chromatographic separation yielded extracts A and B, which were tested against ATP responses at $P2X_1R$ and $P2X_3R$. At $P2X_1R$, extract A was more potent than extract B as an inhibitor of ATP responses (Figure 7a). For extract A, the threshold concentration for blocking activity was 0.1 μM and maximal inhibition occurred at 100 μM. For extract B, the threshold was 3 μM and maximal at 300 μM. IC_{50} (and n_H) values were (mean $\pm$ s.e.m., $n=4$): extract A, 1.4 ± 0.4 μM; extract B, 39.2 ± 5.4 μM (after adjusting for the DMSO effect). These IC_{50} values were significantly different ($P<0.01$). At $P2X_3R$, both extracts were equipotent as antagonists of ATP responses (Figure 7b). The threshold for blockade was 0.3 μM and maximal inhibition occurred at 100 μM. The IC_{50} (and n_H) values were (mean $\pm$ s.e.m., $n=4$): extract A, 5.0 ± 1.7 μM ($n_H=-0.8\pm0.2$); extract B, 4.1 ± 0.8 μM ($n_H=-0.8\pm0.2$). Comparing IC_{50} values, both extracts were more potent than Phenol red Na^+-salt ($P<0.01$).

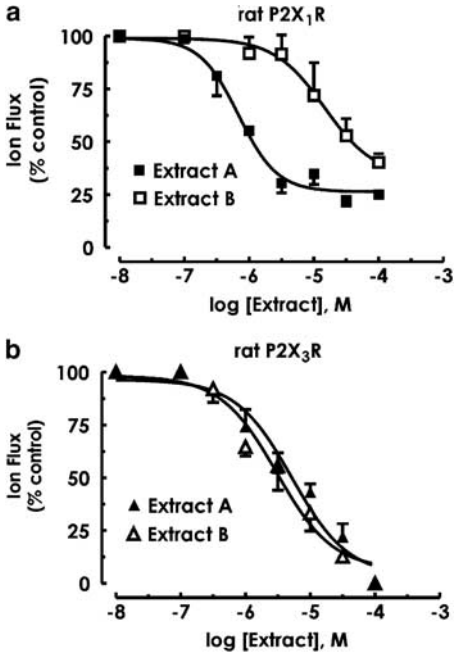

Figure 7 Inhibition curves for lipophilic extracts A and B as antagonists of responses to extracellular ATP (3 μM, the EC_{75}) at rat isoforms of $P2X_1R$ (in a) and $P2X_3R$ (in b). All data points are expressed as mean$\pm$s.e.m. ($n=4$).

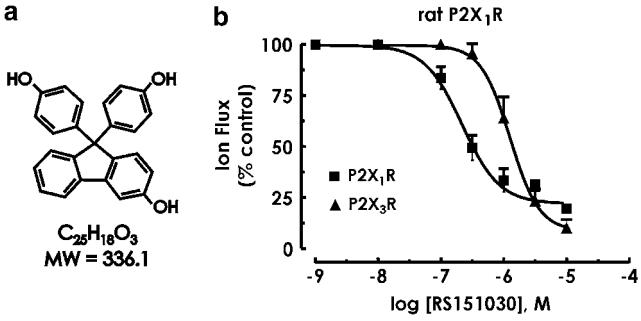

Figure 8 Chemical formula, molecular weight and structure of RS151030 (in a). Inhibition curves for RS151030 antagonism of responses to extracellular ATP (3 μM, the EC_{75}) at the rat isoform of $P2X_1R$ and $P2X_3R$ (in b). All data points are expressed as mean$\pm$s.e.m. ($n=4$).

Blockade by the lipophilic compound RS151030

One compound identified in lipophilic extracts of Phenol red was Compound 5 (9,9-bis[4-hydroxyphenol]-3-hydroxyfluorene) (Figure 8a) (Kym *et al*., 1996). This compound was resynthesised, renamed *RS151030* and tested against ATP responses at P2XRs. At the $P2X_1R$, the threshold concentration for receptor blockade was 0.03 μM, with full blockade at 10 μM (Figure 8b). At the $P2X_3R$, RS151030 was about 10-fold less potent with a threshold of 0.3 μM and full blockade in excess of 10 μM (Figure 8b). After adjusting for the DMSO effect, the IC_{50} (and n_H) values were (mean$\pm$s.e.m., $n=4$): $P2X_1R$, 0.3 ± 0.2 μM ($n_H=-1.0\pm0.2$); $P2X_3R$, 2.4 ± 0.4 μM ($n_H=-1.9\pm0.4$). IC_{50} values for RS151030 were significantly lower ($P<0.05$) than IC_{50} values for Phenol red Na^+-salt at $P2X_1R$ and $P2X_3R$.

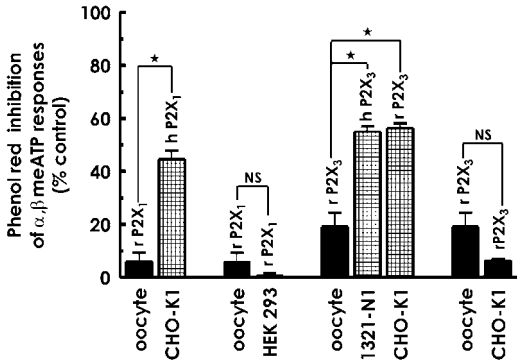

Figure 9 Degree of inhibition of α,βmeATP responses by Phenol red Na^+-salt (100 μM) at P2XR subtypes expressed either in oocytes or mammalian cell lines (CHO-K1, HEK 293 and 1321-N1 cells). Data are expressed as mean$\pm$s.e.m. ($n=4$–9), $^*P<0.05$ (unpaired *t*-test); NS, not significantly different. Solid black bars indicate data from voltage-clamp experiments; lined/hashed bars indicate data from Ca^{2+}-imaging experiments. α,βmeATP (in μM) was applied at the EC_{75} concentration for each P2XR isoform in the following expression systems: (CHO-K1/$hP2X_1R$, 0.1; oocyte/$rP2X_1R$, 3.0; HEK293/$rP2X_1R$, 1.0; 1231-N1/$hP2X_3R$, 0.3; CHO-K1/$rP2X_3R$, 0.3; oocyte/$rP2X_3R$, 3.0; CHO-K1/$rP2X_3R$, 10 μM).

Antagonism of P2XRs in mammalian cells

The antagonist activity of Phenol red Na^+-salt was retested at P2XRs expressed in mammalian cell systems (human $P2X_1R$, in CHO-KI cells; rat $P2X_1R$, in HEK 293 cells; human $P2X_3R$, in 1321-N1cells; rat $P2X_3R$, in CHO-K1). Then, the results from either fluorimetric (FLIPR) or whole-cell current measurements of P2X activation in these expression systems were compared against data from experiments carried out in *Xenopus* oocytes expressing rat orthologues of these P2XRs.

Fluo-3 fluorescence signals, in response to Ca^{2+}-influx caused by α,βmeATP activation of human $P2X_1R$ expressed in CHO-K1 cells, were inhibited by $55\pm3\%$ (mean$\pm$s.e.m.; $n=9$) by Phenol red Na^+-salt (100 μM) (Figure 9). This inhibitory activity was significantly less than the inhibition ($94\pm3\%$, $n=4$) caused by Phenol red Na^+-salt (100 μM) blockade of inward currents evoked by α,βmeATP activation of rat $P2X_1Rs$ expressed in oocytes. With human $P2X_3R$ in 1321-N1 cells or rat $P2X_3R$ expressed in CHO-K1, Phenol red Na^+-salt (100 μM) inhibited in equal measure the Ca^{2+}-stimulated Fluo-3 fluorescence in response to α,βmeATP activation of these $P2X_3R$ subtypes (Figure 9). Here, Fluo-3 signals were inhibited by $45\pm2\%$ (human $P2X_3R$ in 1321-N1; $n=6$) and $44\pm2\%$ (rat $P2X_3R$ in CHO-K1; $n=6$) by Phenol Red Na^+-salt. Yet again, the degree of inhibition was significantly less than the inhibition ($81\pm5\%$, $n=4$) caused by Phenol red Na^+-salt (100 μM) blockade of inward currents evoked by α,βmeATP-activation of rat $P2X_3Rs$ expressed in oocytes.

In a second set of comparative experiments, inward whole-cell currents in response to α,βmeATP activation of GFP-tagged rat $P2X_1R$ expressed in HEK293 cells were completely inhibited by Phenol red Na^+-salt (Figure 9), whereas responses to α,βmeATP activation of rat $P2X_1R$ expressed in oocytes was inhibited almost by the same extent ($94\pm3\%$, $n=4$) by this antagonist. For $rP2X_3Rs$ stably expressed CHO-K1 cells, Phenol red Na^+-salt (100 μM) inhibited α,βmeATP responses by $93\pm1\%$ ($n=3$) (Figure 9), whereas responses to

α,βmeATP activation of rat $P2X_3R$ expressed in oocytes were inhibited by a similar extent, $81 \pm 5\%$ ($n = 4$), by this antagonist.

Thus, in these comparative studies, Phenol red Na^+-salt was active at P2XRs tested in several mammalian expression systems and under all experimental conditions (fluorimetry and patch-clamp). However, when compared to oocyte data, the antagonist was less effective where Ca^{2+}-signals were measured, yet equally effective where inward currents were measured.

Discussion

This investigation revealed that a series of pH-sensitive dyes – principally Phenol red Na^+-salt, but also two lipophilic extracts of Phenol red, the lipophilic compound RS151030, Phenolphthalein base and its K^+-salt – were antagonists of rat P2XRs expressed in oocytes. These compounds showed some selectivity towards the $P2X_1R$ subtype although, in near all cases, they also blocked the $P2X_3R$ subtype with a selectivity window for $P2X_1R$ over $P2X_3R$ of approximately 1 $\log_{10}$-unit of drug concentration. A summary of IC_{50} values at rat $P2X_{1-4}Rs$ is given in Table 1. Furthermore, this investigation demonstrated that the blocking activity of Phenol red Na^+-salt occurred at the concentrations found in culture media (3–50 μM; see Introduction) and that time-dependent blockade also occurred with prolonged exposure to this antagonist. Additionally, Phenol red Na^+-salt displayed antagonist activity at human $P2X_1R$, rat $P2X_1R$, human $P2X_3R$ and rat $P2X_3R$ expressed in mammalian cell lines (CHO-K1, 1321-N1 and HEK 293 cells). To this end, it is advised that future studies of recombinant P2XRs, in heterologous expression systems grown in culture, avoid the use of bathing solutions containing a pH-sensitive red dye – if this is at all possible.

Table 1 Potency of pH-sensitive dyes at rat isoforms of P2XR subtypes

	$P2X_1R$	*$P2X_2R$*	*$P2X_3R$*	*$P2X_4R$*
Phenol red Na^+-salt	3.0	51.9	24.3	Inactive
Phenol red salt (pure)	2.9*	ND	27.6*	ND
	1.00§	ND	17.3§	ND
Phenolphthalein base	1.0¥	>200	17.9	25.8¥
Phenolphthalein K^+-salt	26.1	>200	>200	Inactive
Extract A	1.4¥	ND	5.0	ND
Extract B	39.2¥	ND	4.1	ND
RS151030	0.3¥	ND	2.4	ND

Summary of the mean IC_{50} values (μM) for antagonism of ATP responses at rat isoforms of four P2XR subtypes by the pH-sensitive dyes and lipophilic extracts A and B of Phenol red. For the lipophilic compounds tested, data were corrected by a subtractive process for the activity of solvent DMSO (indicated by the symbol ¥). For purified Phenol red Na^+-salt, the first set of IC_{50} values (indicated by the symbol *) was calculated from inhibition curves and a second set of IC_{50} values (indicated by the symbol §) was calculated from ATP concentration–responses curves showing insurmountable antagonism (ND: not determined).

Finally, the present investigation also revealed that the nonaqueous DMSO had an inhibitory action at $P2X_1R$, and potentiating action at $P2X_4R$. Thus, a measure of caution is also now required when using this solvent in drug studies of these P2XR subtypes.

Compared with other known $P2X_1R$ antagonists – for example, TNP-ATP (Virginio *et al*., 1998), IP_5I (King *et al*., 1999), PPNDS (Lambrecht *et al*., 2000), MRS 2179 (Brown *et al*., 2000), PPADS and its derivative MRS 2257 (Brown *et al*., 2001), and NF449 (Braun *et al*., 2001) – the tested pH-sensitive dyes were not remarkable in terms of their potency. Also, some of the better known $P2X_1R$ antagonists are competitive antagonists and their blocking actions are easily reversed – at least, when used in submicromolar concentrations – whereas purified Phenol red Na^+-salt was an insurmountable antagonist and its blocking actions were not rapidly reversed *in vitro*. The results of assays testing structurally related Phenolphthalein analogues – in either sulphonated or nonsulphonated forms – also failed to reveal a substantial improvement in antagonist potency at the $P2X_1R$. Nonetheless, Phenol red Na^+-salt was found to be as effective as TNP-ATP as an *in vivo* antagonist of purinergic contractions mediated by $P2X_1$-like receptors in the anaesthetised female rat urinary bladder (King *et al*., 2004), whereas $P2X_1R$ antagonists such as IP_5I, PPADS, MRS 2179 and the novel $P2X_1R$ antagonist RO116-6446/008 were much less effective than Phenol red in this model (King *et al*., 2004). Also, it should be borne in mind that Phenol red and other pH-sensitive dyes were antagonists at a number of other P2XR subtypes in addition to $P2X_1R$ and, to this extent, these compounds may still be useful in future experiments on these recombinant P2XR subtypes.

Of the dye compounds investigated, the single most remarkable finding was the blocking activity of Phenolphthalein base at the $P2X_4R$. Since its isolation, the rat isoform of the $P2X_4R$ has been distinguished by its unique refractoriness to blockade by the better known P2 receptor antagonists (e.g. suramin, PPADS and Reactive blue-2; Buell *et al*., 1996). However, the rat isoform can be blocked by TNP-ATP with a mean IC_{50} value of 15 μM and blocked fully at >100 μM (Virginio *et al*., 1998). Phenolphthalein base gave a mean IC_{50} value of 26 μM at rat $P2X_4R$ and showed full blockade at 200 μM. Therefore, in real terms, TNP-ATP and Phenolphthalein base could be considered equipotent – although TNP-ATP, as a nucleotide, is disadvantaged by being dephosphorylated and rendered less potent *in vitro* (Lewis *et al*., 1998) and *in vivo* (Honore *et al*., 2002), whereas Phenolphthalein base is a stable compound and, furthermore, its blocking actions can be reversed with washout. It is hoped that Phenolphthalein base may prove promising as a reversible $P2X_4R$ antagonist *in vivo*. Furthermore, Phenolphthalein base was relatively inactive at $P2X_2R$ and, therefore, this compound could be used to distinguish the slowly desensitising $P2X_4R$ subtype from the $P2X_2R$ *in vivo*. It was also noted that blocking activity at the $P2X_4R$ was lost in the related Phenolphthalein K^+-salt and in Phenol red Na^+-salt which are both sulphonated. The absence of blocking activity by these sulphonated dyes may hold the key to explain the inactivity of many of the better known, yet sulphonated, P2 receptor antagonists at the rat $P2X_4R$. Lastly, Phenolphthalein base has been much used as a stimulant laxative but, in this case, the base must be transformed into an alkaline salt by the

intestine before it can act as an irritant to the colonic mucosa and a stimulant of peristalsis (Cass *et al*., 1965).

At either $P2X_2R$ or $P2X_3R$, none of the tested compounds showed a higher potency than other known P2 receptor antagonists of these subtypes. Thus, Reactive blue-2 remains the most potent antagonist (mean IC_{50}, 0.36 μM) at the rat $P2X_2R$ (King *et al*., 1997) and A317491 is one of the more potent (mean IC_{50}, 0.1 μM) and highly selective antagonists at rat $P2X_3R$ (Jarvis *et al*., 2002). None of the pH-sensitive dyes were tested at either rat $P2X_5R$ or rat $P2X_6R$ because they do not express well in oocytes (King *et al*., 2000; Wildman *et al*., 2002), nor were tested at rat $P2X_7R$ which is difficult to control and also behaves differently from human $P2X_7R$, in terms of the reproducibility of agonist responses, when expressed in oocytes (Petrou *et al*., 1997; Klapperstück *et al*., 2001). Regarding activity at P2YR subtypes, Phenol red Na^+-salt blocked the *Xenopus* $p2y_8R$ with an IC_{50} value of 68 ± 11 μM (mean $\pm$ s.e.m., $n = 4$) (King & Liu, unpublished data) but did not block the human $P2Y_{11}R$ at a concentration up to 100 μM (King & Townsend-Nicholson, unpublished data).

When tested against P2XRs, the lipophilic extracts of Phenol red and Phenolphthalein base required a nonaqueous solvent. DMSO was used but, by itself, showed blocking activity for ATP responses at $P2X_1R$ and a potentiating effect at $P2X_4R$. This is not the first occasion that DMSO has been found to affect ion-channels. At 1% ($v\,v^{-1}$), it selectively diminished acetylcholine responses at the nAChR receptor cloned from *Torpedo* electroplaque, although spared agonist responses at the murine nAChR receptor cloned from skeletal muscle (Eaton *et al*., 1997). Other solvents – including ethanol and toluene at low dilutions (1% $v\,v^{-1}$ and less) – also show either potentiating or inhibitory actions on ATP responses at $P2X_2R$, $P2X_3R$ and $P2X_4R$ (Davies *et al*., 2002; Woodward *et al*., 2004). Therefore, it was not possible to substitute either ethanol or toluene for DMSO as a solvent of lipophilic compounds in the present study.

DMSO was used to dissolve the two lipophilic extracts obtained from the commercially available Phenol red Na^+-salt. Although both lipophilic extracts showed blocking activity at $P2X_1R$ and $P2X_3R$ of similar potency to the salt itself, a sample of the purified and water-soluble Phenol red Na^+-salt was found to retain its blocking activity – without a reduction in potency – and, so, the salt must be considered as the principal pharmacological agent and not these extracts. The lipophilic extracts A and B represent a part of the stated 10% impurity of the commercially available Na^+-salt. It is likely that these extracts contain analogues of the Phenol red base which, except for a sulphone bridge, is similar in structure to Phenolphthalein base. However, the precise chemical nature of all the active compounds present in these two extracts was not elucidated. Nonetheless, one compound now known to be present is the bisphenolic molecule RS151030, which represents about 1% of the total dye content of commercially available Phenol red and about 10% of the lipophilic contamination (Kym *et al*., 1996). This bisphenolic compound proved to be the most potent antagonist of all the dyes tested at $P2X_1R$ and $P2X_3R$.

In summary, pH-sensitive dyes related in structure to Phenol red are antagonists primarily at the rat isoform $P2X_1R$ but are active to varying degrees at other rat and human P2XR subtypes. The base, Phenolphthalein, is additionally a reversible $P2X_4R$ antagonist and shows promise as a substance that might work *in vivo*. The presence of these dyes in culture media – especially for the more commonly used DMEM containing 35 μM Phenol red Na^+-salt – must surely complicate the study of native P2XRs in primary and secondary cultures, and of recombinant P2XRs in heterologous expression systems also bathed in culture media. Thus, it is recommended that culture media containing these red dyes should be avoided if possible in future studies of these LGICs – not only because of the already known oestrogen-like activity of these dyes but also for their ability to block P2XRs.

The financial support of Roche Palo Alto LLC (California, U.S.A.) is gratefully acknowledged. B.F.K. was also funded by BBSRC, U.K., whereas A.T.-N. was funded by BHF, U.K.

References

ASCHRAFI, A., SADTLER, S., NICULESCU, C., RETTINGER, J. & SCHMALZING, G. (2004). Trimeric architecture of homomeric $P2X_2$ and heteromeric $P2X_{1+2}$ receptor subtypes. *J. Membr. Biol.*, **342,** 333–343.

BERTHOIS, Y., KATZENELLENBOGEN, J.A. & KATZENELLENBOGEN, B.S. (1986). Phenol red in tissue culture media is a weak estrogen: implications concerning the study of estrogen-responsive cells in culture. *Proc. Nat. Acad. Sci. U.S.A.*, **83,** 2496–2500.

BINDAL, R.D., CARLSON, K.E., KATZENELLENBOGEN, B.S. & KATZENELLENBOGEN, J.A. (1988). Lipophilic impurities, not phenolsulfonphthalein, account for the estrogenic activity in commercial preparations of phenol red. *J. Steroid Biochem.*, **31,** 287–293.

BRAUN, K., RETTINGER, J., GANSO, M., KASSACK, M., HILDEBRANDT, C., ULLMANN, H., NICKEL, P., SCHMALZING, G. & LAMBRECHT, G. (2001). NF449: a subnanomolar potency antagonist at recombinant rat $P2X_1$ receptors. *Naunyn. Schmiedeberg's Arch. Pharmacol.*, **364,** 285–290.

BROWN, S.G., KIM, Y.C., KIM, S.A., JACOBSON, K.J., BURNSTOCK, G. & KING, B.F. (2001). Actions of a series of PPADS analogs at $P2X_1$ and $P2X_3$ receptors. *Drug Dev. Res.*, **53,** 281–291.

BROWN, S.G., KING, B.F., KIM, Y.C., JANG, S.Y., BURNSTOCK, G. & JACOBSON, K.A. (2000). Activity of novel adenine nucleotide derivatives as agonists and antagonists at recombinant rat P2X receptors. *Drug Dev. Res.*, **49,** 253–259.

BUELL, G., LEWIS, C., COLLO, G., NORTH, R.A. & SURPRENANT, A. (1996). An antagonist-insensitive P2X receptor expressed in epithelia and brain. *EMBO J.*, **15,** 55–62.

CASS, L.J., FREDERIK, W.S. & MONTILLA, E. (1965). Phenolphthalein: a review of the medical literature and a controlled evaluation of its use as a laxative in the treatment of chronic constipation. *Curr. Ther. Res. Clin. Exp.*, **7,** 571–589.

COLLO, G., NORTH, R.A., KAWASHIMA, E., MERLO-PICH, E., NEIDHART, S., SURPRENANT, A. & BUELL, G. (1996). Cloning of $P2X_5$ and $P2X_6$ receptors and the distribution and properties of an extended family of ATP-gated ion channels. *J. Neurosci.*, **16,** 2495–2507.

DAVIES, D.L., MACHU, T.K., GUO, Y. & ALKANA, R.L. (2002). Ethanol sensitivity in ATP-gated P2X receptors is subunit dependent. *Alcohol Clin. Exp. Res.*, **26,** 773–778.

EATON, M.J., PAGAN, O.R., HANN, R.M. & ETEROVIC, V.A. (1997). Differential effects of dimethyl sulfoxide on nicotinic acetylcholine receptors from mouse muscle and *Torpedo* electrocytes. *Neurosci. Lett.*, **230,** 163–166.

ENNION, S.J. & EVANS, R.J. (2001). Agonist-stimulated internalisation of the ligand-gated ion channel $P2X_1$ in rat vas deferens. *FEBS Lett.*, **489,** 154–158.

ERNST, M., SCHMID, C. & FROESCH, E.R. (1989). Phenol red mimics biological actions of estradiol: enhancement of osteoblast proliferation *in vitro* and of type I collagen gene expression in bone and uterus of rats *in vivo*. *J. Steroid Biochem.*, **33,** 907–914.

GRADY, L.H., NONNEMAN, D.J., ROTTINGHAUS, G.E. & WELSHONS, W.V. (1991). pH-dependent cytotoxicity of contaminants of phenol red for MCF-7 breast cancer cells. *Endocrinolology,* **129,** 3321–3330.

GREENBERG, S.S., JOHNS, A., KLEHA, J., XIE, J., WANG, Y., BIANCHI, J. & CONLEY, K. (1994). Phenol red is a thromboxane A2/prostaglandin H2 receptor antagonist in canine lingual arteries and human platelets. *J. Pharmacol. Exp. Ther.,* **268,** 1352–1361.

HONORE, P., MIKUSA, J., BIANCHI, B., MCDONALD, H., CARTMELL, J., FALTYNEK, C. & JARVIS, M.F. (2002). TNP-ATP, a potent $P2X_3$ receptor antagonist, blocks acetic acid-induced abdominal constriction in mice: comparison with reference analgesics. *Pain,* **96,** 99–105.

HOPP, L. & BUNKER, C.H. (1993). Lipophilic impurity of phenol red is a potent cation transport modulator. *J. Cell Physiol.,* **157,** 594–602.

JARVIS, M.F., BURGARD, E.C., MCGARAUGHTY, S., HONORE, P., LYNCH, K., BRENNAN, T.J., SUBIETA, A., VAN BIESEN, T., CARTMELL, J., BIANCHI, B., NIFORATOS, W., KAGE, K., YU, H., MIKUSA, J., WISMER, C.T., ZHU, C.Z., CHU, K., LEE, C.H., STEWART, A.O., POLAKOWSKI, J., COX, B.F., KOWALUK, E., WILLIAMS, M., SULLIVAN, J. & FALTYNEK, C. (2002). A-317491, a novel potent and selective non-nucleotide antagonist of $P2X_3$ and $P2X_{2/3}$ receptors, reduces chronic inflammatory and neuropathic pain in the rat. *Proc. Natl. Acad. Sci. U.S.A.,* **99,** 17179–17184.

JIANG, L.H., KIM, M., SPELTA, V., BO, X., SURPRENANT, A. & NORTH, R.A. (2003). Subunit arrangement in P2X receptors. *J. Neurosci.,* **23,** 8903–8910.

JONES, C.A., VIAL, C., SELLERS, L.A., HUMPHREY, P.P., EVANS, R.J. & CHESSELL, I.P. (2004). Functional regulation of $P2X_6$ receptors by *N*-linked glycosylation: identification of a novel $\alpha\beta$-methylene ATP-sensitive phenotype. *Mol. Pharmacol.,* **65,** 979–985.

KHAKH, B.S., BURNSTOCK, G., KENNEDY, C., KING, B.F., NORTH, R.A., SEGUELA, P., VOIGT, M. & HUMPHREY, P.P. (2001). International Union of Pharmacology. XXIV. Current status of the nomenclature and properties of P2X receptors and their subunits. *Pharmacol. Rev.,* **53,** 107–118.

KING, B.F., KNOWLES, I.D., BURNSTOCK, G. & RAMAGE, A.G. (2004). Investigation of the effects of P2 purinoceptor ligands on the micturition reflex in female urethane-anaesthetized rats. *Br. J. Pharmacol.,* **142,** 519–530.

KING, B.F., LIU, M., BROWN, S.G., KNIGHT, G., TOWNSEND-NICHOLSON, A., DUNN, P.M., WILDMAN, S.S., JACKSON, V.M., CUNNANE, T.C., PFISTER, J., PADILLA, F., FORD, A.P. & BURNSTOCK, G. (2003). P2X receptor blockade by the pH indicator dye, *Phenol red. J. Physiol.,* **547P,** C69.

KING, B.F., LIU, M., PINTOR, J., GUALIX, J., MIRAS-PORTUGAL, M.T. & BURNSTOCK, G. (1999). Diinosine pentaphosphate (IP5I) is a potent antagonist at recombinant rat $P2X_1$ receptors. *Br. J. Pharmacol.,* **128,** 981–988.

KING, B.F., PINTOR, J., WANG, S., ZIGANSHIN, A.U., ZIGANSHINA, L.E. & BURNSTOCK, G. (1996a). A novel P1 purinoceptor activates outward K^+ current in follicular oocytes of *Xenopus laevis*. *J. Pharmacol. Exp. Ther.,* **296,** 93–100.

KING, B.F., TOWNSEND-NICHOLSON, A., WILDMAN, S.S., THOMAS, T., SPYER, K.M. & BURNSTOCK, G. (2000). Coexpression of rat $P2X_2$ and $P2X_6$ subunits in *Xenopus* oocytes. *J. Neurosci.,* **20,** 4871–4877.

KING, B.F., WANG, S. & BURNSTOCK, G. (1996b). P2 purinoceptor activated inward currents in *Xenopus* oocytes. *J. Physiol. (London),* **494.1,** 17–28.

KING, B.F., WILDMAN, S.S., ZIGANSHINA, L.E., PINTOR, J. & BURNSTOCK, G. (1997). Effects of extracellular pH on agonism and antagonism at a recombinant $P2X_2$ receptor. *Br. J. Pharmacol.,* **121,** 1445–1453.

KLAPPERSTÜCK, M., BÜTTNER, C., SCHMALZING, G. & MARKWARDT, F. (2001). Functional evidence of distinct ATP activation sites at the human $P2X_7$ receptor. *J. Physiol.,* **534,** 25–35.

KYM, P.R., HUMMERT, K.L., NILSSON, A.G., LUBIN, M. & KATZENELLENBOGEN, J.A. (1996). Bisphenolic compounds that enhance cell cation transport are found in commercial phenol red. *J. Med. Chem.,* **39,** 4897–4904.

LAMBRECHT, G., RETTINGER, J., BAUMERT, H.G., CZECHE, S., DAMER, S., GANSO, M., HILDEBRANDT, C., NIEBEL, B., SPATZ-KUMBEL, G., SCHMALZING, G. & MUTSCHLER, E. (2000). The novel pyridoxal-5′-phosphate derivative PPNDS potently antagonizes activation of $P2X_1$ receptors. *Eur. J. Pharmacol.,* **387,** R19–R21.

LEWIS, C.J., SURPRENANT, A. & EVANS, R.J. (1998). 2′,3′-*O*-(2,4,6-trinitrophenyl) adenosine 5′-triphosphate (TNP-ATP) – a nanomolar affinity antagonist at rat mesenteric artery P2X receptor ion channels. *Br. J. Pharmacol.,* **124,** 1463–1466.

MULLINS, L.J., TIFFERT, T., VASSORT, G. & WHITTEMBURY, J. (1983). Effects of internal sodium and hydrogen ions and of external calcium ions and membrane potential on calcium entry in squid axons. *J. Physiol.,* **338,** 295–319.

NICKE, A., BAUMERT, H.G., RETTINGER, J., EICHELE, A., LAMBRECHT, G., MUTSCHLER, E. & SCHMALZING, G. (1998). $P2X_1$ and $P2X_3$ receptors form stable trimers: a novel structural motif of ligand-gated ion channels. *EMBO J.,* **17,** 3016–3028.

NORTH, R.A. (2002). Molecular physiology of P2X receptors. *Physiol. Rev.,* **82,** 1013–1067.

NUTTLE, L.C. & DUBYAK, G.R. (1994). Differential activation of cation channels and non-selective pores by macrophage P2Z purinergic receptors expressed in *Xenopus* oocytes. *J. Biol. Chem.,* **269,** 13988–13996.

PETROU, S., UGUR, M., DRUMMOND, R.M., SINGER, J.J. & WALSH JR, J.V. (1997). $P2X_7$ purinoceptor expression in *Xenopus* oocytes is not sufficient to produce a pore-forming P2Z-like phenotype. *FEBS Lett.,* **411,** 339–345.

RAAM, S. (1992). Screening for hybridomas producing antibodies to steroid hormone receptors: interference from phenol red in the hybridoma culture supernates. *Endocrinology,* **131,** 2024–2026.

RETTINGER, J., ASCHRAFI, A. & SCHMALZING, G. (2000). Roles of individual *N*-glycans for ATP potency and expression of the rat $P2X_1$ receptor. *J. Biol. Chem.,* **275,** 33542–33547.

SCHORGE, S. & COLQUHOUN, D. (2003). Studies of NMDA receptor function and stoichiometry with truncated and tandem subunits. *J. Neurosci.,* **23,** 1151–1158.

VALERA, S., HUSSY, N., EVANS, R.J., ADAMI, N., NORTH, R.A., SURPRENANT, A. & BUELL, G. (1994). A new class of ligand-gated ion channel defined by P_{2X} receptor for extracellular ATP. *Nature,* **371,** 516–519.

VIRGINIO, C., ROBERTSON, G., SURPRENANT, A. & NORTH, R.A. (1998). Trinitrophenyl-substituted nucleotides are potent antagonists selective for $P2X_1$, $P2X_3$, and heteromeric $P2X_{2/3}$ receptors. *Mol. Pharmacol.,* **53,** 969–973.

WILDMAN, S.S., BROWN, S.G., RAHMAN, M., NOEL, C.A., CHURCHILL, L., BURNSTOCK, G., UNWIN, R.J. & KING, B.F. (2002). Sensitization by extracellular Ca^{2+} of rat $P2X_5$ receptor and its pharmacological properties compared with rat $P2X_1$. *Mol. Pharmacol.,* **62,** 957–966.

WILDMAN, S.S., KING, B.F. & BURNSTOCK, G. (1999). Modulatory activity of extracellular H^+ and Zn^{2+} on ATP-responses at $rP2X_1$ and $rP2X_3$ receptors. *Br. J. Pharmacol.,* **128,** 486–492.

WOODWARD, J.J., NOWAK, M. & DAVIES, D.L. (2004). Effects of the abused solvent toluene on recombinant P2X receptors expressed in HEK293 cells. *Brain Res. Mol. Brain Res.,* **125,** 86–95.

ZIGANSHIN, A.U., ZIGANSHINA, L.E., KING, B.F. & BURNSTOCK, G. (1995). Characteristics of ecto-ATPase of *Xenopus* oocytes and the inhibitory actions of suramin on ATP breakdown. *Pflügers Archiv.,* **429,** 412–418.

ZIGANSHIN, A.U., ZIGANSHINA, L.E., KING, B.F., PINTOR, J. & BURNSTOCK, G. (1996). Effects of P2 purinoceptor antagonists on degradation of adenine nucleotides by ecto-nucleotidases in folliculated oocytes of *Xenopus laevis*. *Biochem. Pharmacol.,* **51,** 897–901.

(Received August 31, 2004
Revised December 10, 2004
Accepted January 28, 2005)